LA-UR- 09-04972

Approved for public release;
distribution is unlimited.

Title: Influence of Impurities on the Solid-Solid Phase Transitions in Zirconium

Author(s): P. A. Rigg, C. W. Greeff, M. D. Knudson, G. T. Gray, III

Intended for: Shock Compression of Condensed Matter -- 2009
AIP Press

Los Alamos
NATIONAL LABORATORY
EST. 1943

INFLUENCE OF IMPURITIES ON THE SOLID-SOLID PHASE TRANSITIONS IN ZIRCONIUM

P. A. Rigg*, C. W. Greeff†, M. D. Knudson and G. T. Gray, III‡**

*Los Alamos National Laboratory, PO Box 1663, MS P952, Los Alamos, NM 87545
†Los Alamos National Laboratory, PO Box 1663, MS B221, Los Alamos, NM 87545
**Sandia National Laboratories, New Mexico, PO Box 5800, Albuquerque, NM 87185-1195
‡Los Alamos National Laboratory, PO Box 1663, MS G755, Los Alamos, NM 87545

Abstract. In an effort to better understand the influence of impurities on the solid-solid phase transitions in Group IVb metals, experiments have been carried out on polycrystalline zirconium samples using plate impact and isentropic loading techniques. Samples with three levels of impurities were shock-loaded using both gas and powder-driven guns and isentropically loaded using magnetic drive (Sandia's Z-Machine) to determine the properties and characteristics of both the $\alpha \rightarrow \omega$ and $\omega \rightarrow \beta$ transitions.

Keywords: zirconium, phase transitions, plate impact, isentropic compression
PACS: 47.40.Nm, 62.50.Ef, 64.70.K, 81.70.Bt

INTRODUCTION

Zirconium can exsist in three solid phases commonly referred to as α (hcp), β (bcc), and ω (hex-3). Figure 1 shows the calculated phase diagram for Zr [1] for the three solid phases with an overplot of the experimentally determined Hugoniot [2–4]. As indicated in the figure, both high-pressure solid phases are accessible through shock compression experiments. The isentrope will lie below the Hugoniot in this figure and therefore, we expected to be able to access the transitions through isentropic compression experiments as well. The purpose of this study is to investigate how the $\alpha \rightarrow \omega$ and $\omega \rightarrow \beta$ phase boundaries change with added impurities and what effects — if any — they have on the kinetics of this phase change.

EXPERIMENTAL METHOD

To investigate the influence of impurities on the $\alpha \rightarrow \omega$ and $\omega \rightarrow \beta$ phase transisions in zirconium, both shock and isentropic compression experiments were performed on samples with three different im-

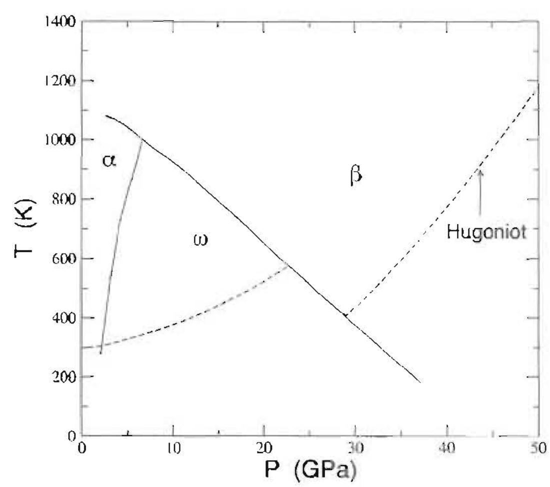

FIGURE 1. Calculated zirconium Hugoniot and phase diagram.

TABLE 1. Impurity levels (ppm) for the three types of Zr samples used in these experiments.

Sample	O	Hf	Fe	N	C
Zr_0	<50	<50	<50	<20	22
Zr_I	390	350	125	15	70
Zr_{II}	1,200	14,000	2,400	80	270

purity levels. The recent paper by Cerreta, *et. al.* [5] argued that the presence of oxygen — which occupies interstitial sites within the zirconium lattice — has the largest influence on the $\alpha \rightarrow \omega$ phase transition. In that study, samples with three distinct levels of oxygen were examined using shock and quasi-static compression experiments. It was found that a relatively small amount of oxygen could raise the transition stress significantly under shock compression experiments and that larger amounts of oxygen seemed to inhibit the transition completely. Here, we extend the shock compression work presented earlier [5] to higher stresses to look for the $\alpha \rightarrow \omega$ transition in the least pure sample as well as the $\omega \rightarrow \beta$ transition in the two least pure materials. The samples studied here originated from the same large plate materials used previously [5]. A summary of of the main impurities in each material is summarized in Table 1. Throughout the remainder of the text, we will refer to the materials as they are labeled in this table with Zr_0 representing high purity crystal-bar Zr.

Shock compression experiments were performed at Los Alamos National Laboratory using a gas-driven 50 mm gun and a 40 mm powder-driven gun. All samples were prepared as disks 38 mm and 32 mm in diameter for the gas- and powder-gun experiments, respectively. The samples – 3 to 6 mm thick and backed by 19 mm thick sapphire or LiF windows – were impacted with various materials to produce peak stresses up to 41 GPa. This is shown schematically in Fig. 2(a). Isentropic loading experiments to roughly 47 GPa peak stress were performed at Sandia National Laboratory using the Z-Machine [6, 7] with samples roughly 0.5 mm thick and 10 mm in diameter and backed by 6 mm thick LiF or sapphire windows as shown in Fig 2(b). VISAR [8] was used in all experiments to measure the particle velocity at the sample/window interface.

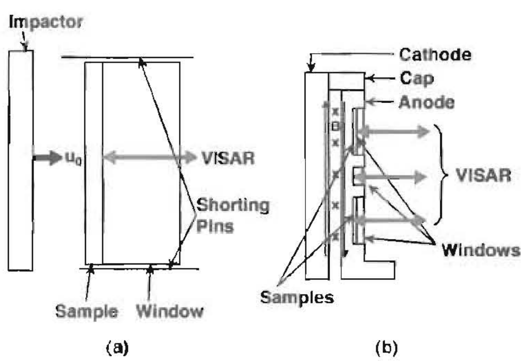

FIGURE 2. Experimental configurations used for (a) shock compression and (b) isentropic compression experiments.

RESULTS

Figure 3 shows direct comparison of the wave profiles obtained for the three types of samples when shock-compressed above the $\alpha \rightarrow \omega$ phase transition stress. Because both LiF and sapphire windows were used in these experiments, the particle velocity data obtained using VISAR were converted to stress data using a simple impedance matching calculation to compare the wave profiles more readily. In these experiments, multiple wave structure is seen in all three materials. The first, low amplitude, wave is the elastic precursor which is similar for all three materials. The final two waves are commonly referred to as the P1 and P2 waves representing shock propagation in the parent and daughter phases, respectively. As can be seen in the figure, the transition in the Zr_I material is almost 1 GPa higher than the transition in the Zr_0 material, while the transition in the Zr_{II} material is over 4 GPa higher still. The wave profile from the Zr_{II} experiment is also very different from that observed for the other two materials. Despite the fact that the Zr_{II} sample was twice the thickness of the Zr_0 and Zr_I samples, no clear separation between the P1 and P2 waves was observed. The only evidence that the phase transformation has occurred is a transition from a square wave profile below the phase transformation to a more rounded profile above the transformation. Furthermore, the P2 wave was easily overdriven just a few GPa higher, in contrast to the Zr_0 and Zr_I experiments.

The results of the quasi-isentropic experiments performed on Sandia's Z-machine at 40 GPa are

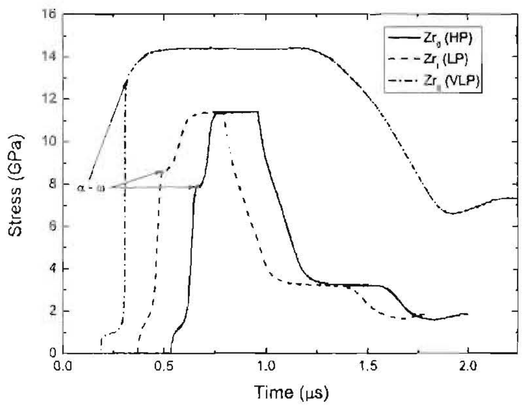

FIGURE 3. Partical velocity wave profiles (converted to stress) from shock compression experiments performed on the three types of Zr at peak stresses above the $\alpha \rightarrow \omega$ phase transition.

shown in Fig. 4. Three distinct kinks are observable in each of the profiles. Again, the velocity data were converted to stress using impedance matching. The first kink near the bottom of each record is due to the shape of the current pulse used in the Z-Machine to generate the ramp waves in each sample, but also shows evidence of the elastic precursor. The second kink is attributed to the $\alpha \rightarrow \omega$ phase transition. Although the transition stresses for each material seem to be higher in the isentropic compression experiments than in the shock compression experiments, similar differences in the transition stress between the three materials are observed in both cases. However, in stark contrast to the gun experiments, the transition is much more pronounced in the Zr_{II} material than in the other two materials. At this time, it is not understood why this difference is observed, but in general, it suggests that the large amount of oxygen present in the Zr_{II} material is significantly changing the kinetics of the $\alpha \rightarrow \omega$ transition and could also be affecting the equation of state of this material. Furthermore, isentropic compression experiments performed at a lower peak stress resulted in lower transition stresses for each material. We believe this is also due to the kinetics of this transition. Further details about the $\alpha \rightarrow \omega$ transition experiments can be found elsewhere [9] including comparison of experimental results to calculations using the kinetic model developed by Greeff [11]. The third kink seen in the data shown in Fig. 4 is attributed to the $\omega \rightarrow \beta$ tran-

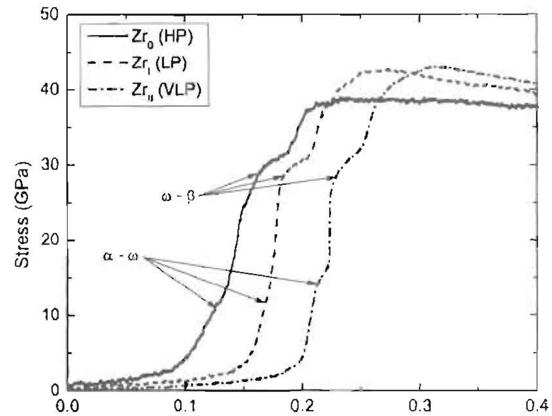

FIGURE 4. Partical velocity wave profiles (converted to stress) from isentropic compression experiments performed on the Sandia Z-Machine at peak stresses above the $\omega \rightarrow \beta$ transition.

sition, but unlike the $\alpha \rightarrow \omega$ transition, the $\omega \rightarrow \beta$ transition stress does not seem to be influenced by impurity concentration.

Based on Fig. 1, we expected to see multi-wave structure due to the $\omega \rightarrow \beta$ transition in shock compression experiments to occur somewhere between 22 and 24 GPa. As expected, experiments conducted on Zr_I and Zr_{II} samples showed no evidence of a phase transition below 22 GPa. However, experiments conducted between 22 and 41 GPa also failed

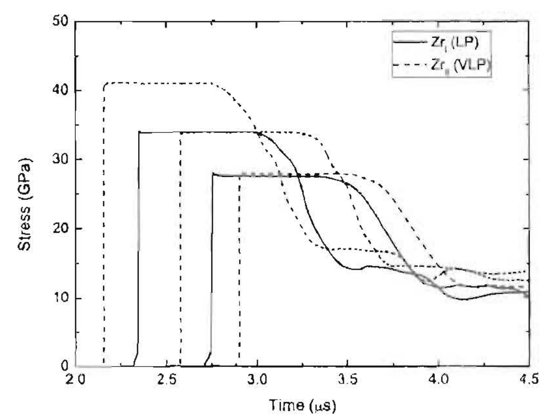

FIGURE 5. Partical velocity wave profiles (converted to stress) for shock compression experiments performed on Zr_I (solid lines) and Zr_{II} (dashed lines) samples between 26 and 41 GPa.

to reveal multi-wave structure indicative of a phase transition. Fig. 5 shows the wave profiles obtained from experiments with peak stresses between 26 and 41 GPa. The two lowest stress experiments in this figure show evidence of a slight overshoot followed by relaxation that may be an indicator that the phase transition is occurring, but the feature disappears at stresses just a few GPa higher.

CONCLUSIONS

Shock and quasi-isentropic compression experiments were performed on Zr samples containing three different levels of impurities. These experiments revealed the $\alpha \rightarrow \omega$ transiton in all three materials under shock and isentropic compression and demonstrated that the addition of small amounts of impurities in the Zr resulted in dramatic differences in both the transition stress and kinetics of the $\alpha \rightarrow \omega$ phase transformation. Furthermore, this transition occurs much higher than the calculated equilibrium transition stress shown in Fig. 1 for all three materials and both loading techniques. A kinetic model that describes this behavior in zirconium has been developed by Greeff [1] with comparisons of wave profiles calculated using this model to experimental data can be found in the manuscript by Rigg, *et. al.* [9]. In addition, the $\omega \rightarrow \beta$ transition was observed in the isentropic compression experiments at approximately 30 GPa for all three materials indicating that the presence of impurities in zirconium has no effect on transformation to the β phase. This transition was not observed in the shock compression experiments performed in a stress range spanning both below and above this stress and further experiments are needed to determine where the transition occurs under shock loading. This work has demonstrated that performing both shock and isentropic compression experiments can provide information that neither technique can provide alone and will lead to a better understanding of the equation of state of materials that undergo solid-solid phase transformations under dynamic loading conditions.

ACKNOWLEDGMENTS

We would like to thank Mark Byers, Frank Abeyta, Tim Pierce, and James Esparza for building and assisting with the execution of the plate impact experiments described in this manuscript. The many folks at Sandia National Laboratory responsible for reliable operation of the Z-Machine are also thanked for assisting with the isentropic compression experiments. This work was performed under the auspices of the U.S. Department of Energy.

REFERENCES

1. Greeff, C. W., *Modelling Simul. Mater. Sci. Eng.*, **13**, 1015 (2005).
2. Walsh, J. M., Rice, M. H., McQueen, R. G., and Yarger, F. L., *Phys. Rev.*, **75**, 196 (1957).
3. Rice, M. H., McQueen, R. G., and Walsh, J. M., *Solid State Physics, Vol. 6*, Academic Press, New York, 1958.
4. McQueen, R. G., Marsh, S. P., Taylor, J. W., Fritz, J. N., and Carter, W. J., *High Velocity Impact Phenomena*, Academic Press, New York, 1970.
5. Cerreta, E., Gray III, G. T., Hixson, R. S., Rigg, P. A., and Brown, D. W., *Acta Materialia*, **53**, 1751 (2005).
6. Hall, C. A., Asay, J. R., Knudson, M. D., Stygar, W. A., Spielman, R. B., Pointon, T. D., Reisman, D. B., Toor, A., and Cauble, R. C., *Rev. Sci. Instrum.*, **72**, 3587 (2001).
7. Hall, C. A., *Phys. Plasmas*, **7**, 2069 (2000).
8. Barker, L. M., and Hollenbach, R. E., *J. Appl. Phys.*, **43**, 4669 (1972).
9. Rigg, P. A., Greeff, C. W., Gray III, G. T., Hixson, R. S., and Knudson, M. D., Influence of impurities on the α to ω phase transition in zirconium under dynamic loading conditions (2009), submitted to J. Appl. Phys.